Desalination and Water Treatment
www.deswater.com

doi:10.5004/dwt.2017.20188

66 (2017) 80–87
March

Synthesis of intermediate crystal $Ba_{1-x}Ca_xSO_4$ system via co-precipitation of $BaSO_4$-$CaSO_4$ and partial hindrance of gypsum formation

Hanen Azaza[a], Amira Doggaz[a], Lassaad Mechi[a,*], Virgil Optasanu[b], Mohamed Tlili[a], Mohamed Ben Amor[a]

[a]*Water Researches and Technologies Center, Borj-Cedria Technopark, Tourist Route of Soliman, PO-box N°273 – 8020, Soliman, Nabeul, Tunisia, email: azaza.hanen@yahohoo.fr (H. Azaza), amira.doggaz@yahoo.com (A. Doggaz), mechilassaad@yahoo.fr (L. Mechi), mohamed.tlili@certe.rnrt.tn (M. Tlili), mohamed.benamor@certe.rnrt.tn (M.B. Amor)*
[b]*Département Génie Mécanique et Productique. Université de Bourgogne, IUT de Dijon, email: virgil.optasanu@u-bourgogne.fr*

Received 2 March 2016; Accepted 20 August 2016

ABSTRACT

During the production of hydrocarbons from subterranean reservoirs, calcium sulphate and barium sulphate scaling cause flux decline and dangerous problems in production facilities. Numerous studies have investigated the single salt precipitation in aqueous media. This work is intended to study the co-precipitation of $BaSO_4$-$CaSO_4$, commonly observed salts in the oil sector. The conductometric method was used to follow the progress of the co-precipitation reaction of $CaCl_2$-Na_2SO_4-barite suspension and $BaCl_2$-$CaCl_2$-Na_2SO_4 aqueous solutions at acid and alkaline medium. The obtained precipitates were characterized by FTIR, RAMAN, SEM, EDX and XRD. In $CaCl_2$-Na_2SO_4-barite suspension solution, experiments have showed no difference in gypsum precipitation mode. For $BaCl_2$-$CaCl_2$-Na_2SO_4 solution at acid medium, it was shown that during the co-precipitation reaction, intermediate mixed crystals $Ba_{1-x}Ca_xSO_4$ can be formed with an induction ***time increases in comparison to pure gypsum nucleation***. Intermediary solids, which precipitate in dendritic shape, crystallize in both orthorhombic ($x < 0.5$) and monoclinic ($x > 0.5$) systems through an insertion and substitution mechanism of calcium in the crystal lattice of barites. Nevertheless, at alkaline medium (pH 8.3), the results have revealed that the presence of Ba^{2+} has not a significant effect on gypsum precipitation kinetics.

Keywords: Barite, Co-precipitation of $BaSO_4$-$CaSO_4$, Intermediate solids $Ba_{1-x}Ca_xSO_4$, Morphology, Structure.

1. Introduction

The precipitation of inorganic salts, such as barium sulphate, calcium carbonate, calcium sulphate, from produced brines is a persistent and common problem encountered during the production of hydrocarbons from subterranean reservoirs, as a result of variation in chemical and thermodynamic parameters.

Scale deposition in the reservoir and in production equipment is a common problem during enhanced oil recovery operations involving water flooding or a water drive. The mixture of incompatible fluids, containing various ions, is the main reason leading to more salts precipitation, which might be combined to form tartar. Crystals then stick to the pipe wall, forming an insoluble and very compact deposit which can cause irreversible and dangerous damage for pipelines and production facilities.

The alkaline earth sulphates and carbonates scales including $SrSO_4$, $CaCO_3$, $CaSO_4$ and $BaSO_4$ scales are the major scaling contributors in oil production [1]. Having regard to its low solubility, barium sulphate is the main disturbance in oil equipments and it casts instantly when water, rich in sulphates, is mixed with barium-rich water. This is the case of certain water deposits (such as Zarzaitine or Hassi Massaoud) containing barium salts.

*Corresponding author.

Both calcium and barium sulphate scales are sulphate scales. Most of studies investigated barium sulphate and calcium sulphate on a single scale deposition [2–4]. Many researchers have studied thermodynamics and kinetics of calcium carbonate and calcium sulphate co-precipitation to understand the mutual effect between these two salts [5–8]. Mulopo (2015) [9] has studied $BaCO_3$-$CaSO_4$ system in desalination process during an acid mine drainage treatment.

Zhu [10] has provided a theoretical evaluation of co-precipitation and fundamental data of binary mixing ($BaSO_4$-$SrSO_4$, $BaSO_4$-$RaSO_4$, $BaSO_4$-$PbSO_4$, and $SrSO_4$-$PbSO_4$) properties in the barite isostructural family. Liu et al. [7] and Naseri et al. [11] have demonstrated that $BaSO_4$ and $CaSO_4$ co-deposition was so different compared to each $BaSO_4$ or $CaSO_4$ deposition in porous media at different temperatures.

In this research, we investigate the $BaSO_4$-$CaSO_4{\cdot}2H_2O$ co-precipitation. So, we present a comprehensive study on the effect of pH, barium cation and $BaSO_{4(sd)}$ on the barite-gypsum co-precipitation. This includes a morphological and structural analysis of crystal compounds in the system $BaSO_4$-$CaSO_4$-H_2O.

2. Materials and experimental procedure

2.1. Materials

In order to explore the co-precipitation reaction, an experimental unit was used and it is represented in Fig. 1. One liter closed thermostatic cell was used to maintain the solution at constant temperature by a thermostatic liquid circulation (303 K). The magnetic stirrer was used to keep the solution homogeneous. The solution pH and conductivity parameters were measured using Proline B 210 pH-meter and a Proline B 250 conductivity cell.

2.1.1. Chemicals reagents

Barium chloride ($BaCl_2{\cdot}2H_2O$), calcium sulphate ($CaSO_4$), calcium chloride, ($CaCl_2{\cdot}2H_2O$) and NaOH were used for an analytical grade supplied by SIGMA-ALDRICH and FLUKA.

- In solid XRD phase identification we have exerted The HighScore software.

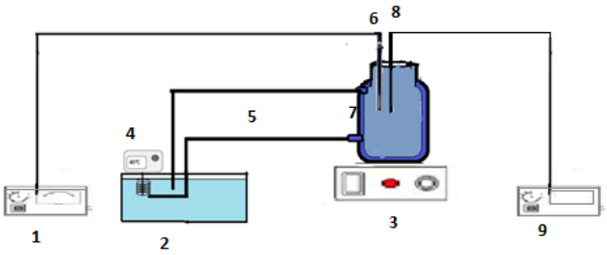

Fig. 1. Experimental unit: 1. Conductivity cell using Proline B 250; 2. Thermostatic bath; 3. Magnetic stirrer; 4. Heating head; 5. Pipes; 6. Electrode conductivity; 7. Double-wall reactor of 1000 ml; 8. Electrode pH; 9. pH meter Proline B 210.

- In the structural profile refinement, we have used FullProf software [12]. The FullProf program is formed by a set of crystallographic programs (FullProf, WinPLOTR, EdPCR, GFourier, etc.) mainly developed for Rietveld analysis of neutron or X-ray powder diffraction data collected at constant or variable step in scattering angle 2theta.

2.2. Experimental procedure

The experimental protocol performed for these reactions was carried out in two different operating modes.

- Mode 1: Adding an amount of barite seeds to supersaturated $CaSO_4{\cdot}2H_2O$ solutions at T = 303 K. So, we have prepared four solutions in order to study the co-precipitation phenomenon. (Table 1).
- Mode 2: The supersaturated solutions of barium sulphate and calcium sulphate were prepared by mixing dissolved $BaCl_2{\cdot}2H_2O$ and $CaCl_2{\cdot}2H_2O$ in 500 mL of distillated water with 500 mL of Na_2SO_4 at T = 303 K. The manipulation was performed at an acid pH (5.5) and an alkaline pH (8.3).

The solid phase got, was analyzed by FTIR, XRD, SEM and Raman spectroscopy. Infrared spectra of the samples in KBr pellets were obtained by defusing reflectance by accumulating 40 scans on an Affinity-1C Schimadzu spectrophotometer, in the range of 4000–400 cm^{-1} with 4 cm^{-1} of resolution. Micro Raman spectrometry examination was obtained by using a Jobin Yvon High Resolution Raman Spectrometer (brand: HORIBA Jobin Yvonet model: LabRam HR). Micro-Raman spectra were obtained with a LABRAM spectrometer (ISA-Jobin Yvon). XRD is carried out at room temperature with a Philips X'PERTPRO diffractometer in step scanning mode using Cu Kα radiation (λ = 0.15418 nm). The XRD patterns were recorded in the scanning range 2 h = 5–90°. A small angular step of 2h = 0.017° and fixed counting time of 4 s were used. The XRD reflection positions were determined using 'X-Pert HighScore Plus' software

3. Theoretical background

Pure gypsum and pure barite precipitation are accorded to the two following reactions:

$$Ca^{2+} + SO_4^{2-} + 2H_2O \rightarrow CaSO_4 \cdot 2H_2O \quad \text{R.1}$$

$$Ba^{2+} + SO_4^{2-} \rightarrow BaSO_4 \quad \text{R.2}$$

Precipitation occurs only if the ionic activities product (IAP) exceeds the solubility constant (K_{sp}). Knowing that the super-saturation is the driving force for the crystallization, nucleation and crystal growth are initiated when the supersaturation coefficient (), defined us the ratio between the IAP and K_{sp}, in the solution is greater than 1. Supersaturation coefficient was than calculated as follow for gypsum and barite as references, without considering the formation of any other solids in the solution:

$$\Omega_{gypsum} = \frac{\gamma_{Ca^{2+}}\left[Ca^{2+}\right]\gamma_{SO_4^{2-}}\left[SO_4^{2-}\right]\gamma^2_{H_2O}\left[H_2O\right]^2}{K_{sp.gypsium}} \quad (1)$$

Table 1
Solutions used in the present experimental study

	$[Ca^{2+}]$ (M)	$[SO_4^{2-}]$ (M)	Mode 1:m_{BaSO_4} (g)		Mode 2:$[Ba^{2+}]$ (M)	
Experiment a	4.47×10^{-2}	4.47×10^{-2}	0	pH = 5.5	0	pH = 5.5
Experiment b	4.47×10^{-2}	4.47×10^{-2}	0.07	pH = 5.5	3.10^{-4}	pH = 5.5
Experiment c	4.47×10^{-2}	4.47×10^{-2}	0.7	pH = 5.5	10^{-3}	pH = 5.5
Experiment d	4.47×10^{-2}	4.47×10^{-2}	1.7	pH = 5.5	10^{-3}	pH = 8.3

$$\Omega_{BaSO_4} = \frac{\gamma_{Ba^{2+}}\left[Ba^{2+}\right]\gamma_{SO_4^{2-}}\left[SO_4^{2-}\right]}{k_{sp,BaSO_4}} \quad (2)$$

where [ ] represents the molar concentration of the subscripted aqueous free species, K_{sp} refers to the solubility constant, γ_i defines the ionic activity coefficient of the subscripted aqueous species.

For T =303 K:$k_{sp,CaSO_4} = 4.25 \times 10^{-5}$ [13] and $k_{sp,BaSO_4} = 1.14\ 10^{-10}$ [14].

γ_i is calculated as function of the ionic strength I by the following equation [15].

$$\log \gamma_i = -AZ_i^2\left(\frac{\sqrt{I}}{1+\sqrt{I}} - 0.3I\right) \quad (3)$$

where $A = 1.82 \times 10^6 (\varepsilon T)^{\frac{-3}{2}}$, ε is the dielectric constant of water and T is the temperature in K.

In the following and throughout the text, the supersaturation coefficient (Ω) that will be presented is calculated from ions species concentrations present in the solution at time $t = 0$ before any solid formation.

4. Results and discussion

Gypsum and sulphate crystals crystallization in presence of barium (mode 1 and mode 2), based on conductivity measurements and integrated by a morphological and structural investigation is here presented.

Seeing that the solution composition differs for each experiment and in order to compare results, it was chosen to present the Δσ conductivity instead of the solution conductivity curves. Delta conductivity (Δσ) is the difference between the initial conductivity and the conductivity at the time t: $\Delta\sigma = \sigma_{initial} - \sigma_t$.

4.1. Mode 1: Effect of barite seeds on gypsum precipitation

Fig. 2 shows the precipitation curves in $CaCl_2$-Na_2SO_4-barite suspension. It illustrates that in mode 1, the presence of the amount of $BaSO_{4(sd)}$ did not present any significant effect on pure gypsum precipitation. All curves present two zones; the first one extends from the beginning of the precipitation test ($t = 0$) to the induction time where the conductivity slope change. This zone can be attributed to the nucleation step. The second zone, after the induction time, corresponds to the growth step of gypsum. Whatever the added barite amount is, all precipitation curves remain superposed during the nucleation and the first step of growth. So, it can be concluded that the presence of barite crystals did not play the role of a precursor of $CaSO_4{\cdot}2H_2O$ precipitation which forms in bulk solution and not on barite surface.

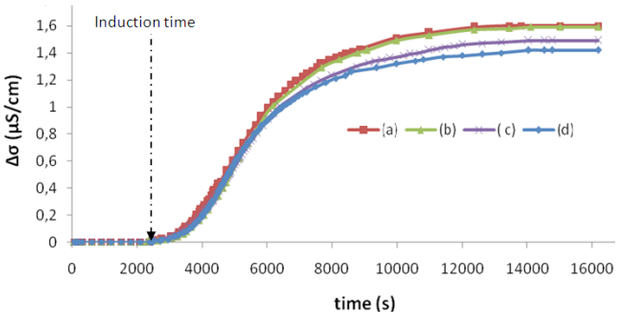

Fig. 2. Temporary delta conductivity variation ($\Delta\sigma = \sigma_{initial} - \sigma t$) in gypsum supersaturated solution with: a) $m_{BaSO_4} = 0$, b) $m_{BaSO_4} = 0.07$ g and c) $m_{BaSO_4} = 0.7$ g and d) $m_{BaSO_4} = 1.7$ g ($\Omega_{gypsum} = 6$, T= 303 K, pH = 5.5).

4.2. Mode 2: Effect of barium ions on sulphate crystals precipitation

4.2.1. In acid medium pH=5.5:

Fig. 3 shows the precipitation curves in the $CaCl_2$-Na_2SO_4-$BaCl_2$ solution in an acid medium. Mode 2 exhibits a different trend with different concentration of Ba^{2+} ion. The precipitation kinetic seems significantly affected in a Ba^{2+} rich solution. It increases the *induction time* which passes from 2700 s to 3800 s in presence of 3.10^{-4} M of Ba^{2+}. By adding 10^{-3} M, the induction time passes to 6000 s. The best of our knowledge shows that no previous research study has revealed similar results.

Seeing that barite is less soluble than gypsum ($k_{sp,CaSO_4} = 4.25 \times 10^{-5}$ and $k_{sp,BaSO_4} = 1.14 \times 10^{-10}$); although the low barium content (Table 1), the solution remain more supersaturated regarding barite then gypsum. So, barite precipitates at first. Nevertheless, comparing results of Figs. 2 and 3 permits to conclude that barite was not formed in the present experimental conditions. This was confirmed during solid characterization whose results will be presented below. Indeed, barite cannot significantly affect gypsum precipitation kinetics (Fig. 2).

So we may conclude that co-precipitation is occurring and not a heterogeneous nucleation of gypsum on barite. The co-precipitation determines an apparent decrease of the supersaturation in respect to gypsum and an increase of its induction time for nucleation.

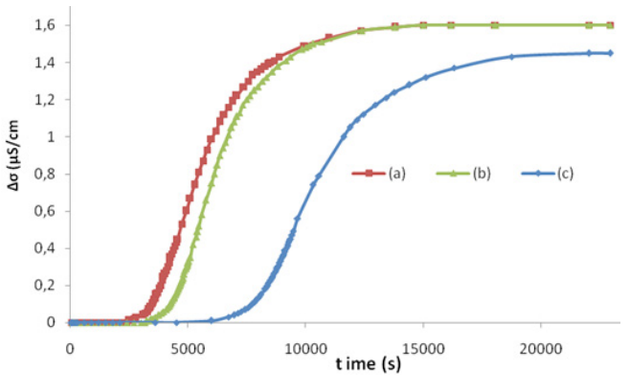

Fig. 3. Temporary delta conductivity variation ($\Delta\sigma = \sigma_{initial} - \sigma t$) at 303 K in gypsum supersaturated solution with: a) $[Ba^{2+}] = 0$ M, b) $[Ba^{2+}] = 3.10–4$ M and c) $[Ba^{2+}] = 10\times10^{-4}$ M. ($\Omega_{gypsum} = 6$, T = 303 K, pH = 5.5).

In order to explain this difference, precipitates were collected at three different points in experience (c) (Fig. 3) and identified. The compound (1) was collected at $t = 1500$ s before the slope change. The second sample, compound (2), was collected after 6800 s from the beginning of the precipitation test; and the third solid, compound (3), was recovered at the end of the experience. Solid analyses are presented in Figs. 4–7.

Fig. 4 illustrates IR and Raman spectra and XRD pattern of the compound (1) and the pure barite, synthesized at laboratory scale, as reference. IR spectra have shown many differences in the spectrum of the compound (1) with respect to the pure barium sulphate. A small shift of about 4 cm^{-1} of the band corresponding to the out-of-plane bending vibration of the SO_4 at 638 cm^{-1} [16] was recorded. Moreover, barite is characterized by the three bands of sulphate ion vibration located at 1070; 1114; 1197 cm^{-1} according to the sulfur-oxygen (S-O) stretching [16]; whereas the compound (1) spectra shows only two bands in this region located at 1070 and 1163 cm^{-1} . This lets suggest that the compound (1) is a sulphate different from barite.

Raman analysis (Fig. 4.B) confirms that the compound (1) and barite have different microstructure. The most intense vibration band of the sulphate ion was shifted by about 3 cm^{-1} with a broadening. Similar results were recorded in the case of calcium carbonate precipitated in presence of Mg^{+2} [17] and in a Raman spectroscopic studies of the $BaSO_4$–$SrSO_4$ binary series [18]. A shift of the band of carbonate vibration in calcite from 1075 cm^{-1} to 1077 cm^{-1} was recorded. This was attributed to the crystallization of magnesian calcite $Ca_{1-x}Mg_xCO_3$ [17]. At light of the literature and seeing the lower radius of calcium ion regarding to the barium ion, the shift recorded in IR and Raman spectra can be attributed to a substitution of Ba^{+2} by Ca^{+2} or insertion of Ca^{2+} in the barite lattice to form a solid solution $Ba_{1-x}Ca_xSO_4$.

The X-ray characterization (Fig. 4C) shows a net difference between the diffraction patterns of the two solids: compound (1) and pure barium sulphate. Indeed, we noticed that the most intense peaks were moved towards increasing θ. In fact, the diffraction peak of the plane (2 1 0), the most intense one (normalized to 100%), located at 2θ = 25.81° shifted to 2θ = 26.66°. This confirms IR and RAMAN analyses showing that compound (1) and barite are different. The peak shift towards higher 2θ angles is due to the barite lattice distortions caused by the presence of calcium. Indeed, Ca^{2+} can form part of the lattice of the barite by substituting the Ba^{2+} ions. The ion radius of Ca^{2+} (1.97 Å) is smaller than that of Ba^{2+} (2.24 Å). This involves a compression of the crystal lattice which results in a shift of the XRD peaks. The lattice parameters calculated using the software fulproof are collected in Table 2. It shows that this substitution leads to the unit cell volume (v) decrease from 69300 $Å^3$ to 669.18 $Å^3$.

Table 2 depicts the structural parameters of compounds (1) and (2). The refinement of the diffraction pattern was made with foolproof software allowed us to determine the crystal system and the lattice parameters of the unit cell.

We have: Chi 2 which represents Global user-weigthed (Bragg contribution), and R-Factor that refers to reliability factor.

$$R_F = \sum_{hkl} |F_{hkl}(\text{obs}) - F_{hkl}(\text{calc})| / \sum_{hkl} |F_{hkl}(\text{obs})|$$

F is the so-called structure factor

R-factor is less than 4%, which shows an agreement between the crystallographic model and the experimental X-ray diffraction data.

Beside peaks shift, the XRD pattern of the compound (1) shows, regarding to the barite XRD pattern, additional peaks (e.g. at 2θ = 33.61° and 40.37°) and a disappearance of some peaks (e.g. at 2θ = 19.98° and 47.01°) which can be attributed to the insertion of Ca^{2+} in the barite lattice. The identification of the compound (1) by HighScore software indicates that it is very similar to $Ba_{0,6}Ca_{0,4}SO_4$ [19] compound which was crystallized in the same crystal system (orthorhombic) as barite (Table 2). This confirms the substitution, and/or insertion of calcium in barite lattice to form a solid solution $Ba_{1-x}Ca_xSO_4$. The same phenomenon has been observed in case of $BaCl_2$-Sr-Cl_2-Na_2SO_4-system where the solid phase which has been obtained is $Ba_{1-x}Sr_xSO_4$ [20].

Micrographic EDX (energy dispersive X-ray spectroscopy) analysis (Table 3) indicated that Ba^{2+} is about 80% and Ca^{2+} 20%. For that, the statistic formula of compound (1) is $Ba_{0.8}Ca_{0.2}SO_4$.

SEM image (Fig. 5) shows that the presence of calcium in barite lattice affects the precipitate morphology. The morphology of barite which was rhomboedric [21] has transformed in dendritic when the solid is $Ba_{1-x}Ca_xSO_4$.

The arms of the dendrites grew in parallel with favorable growth direction. Studies have been carried out taking into account the anisotropy of the interfacial energy γ [22–25] to explain the dendrite growth. A seed stem first grows quite rapidly, and at a later stage primary branches will grow out of the stem at a slower rate. Dendrite growth is a result of kinetic anisotropy attachment or nucleation anisotropy. In our experimental condition, the dendretic growth can be attributed to the anisotropy of the interfacial energy γ by adsorption of calcium ions on barite nuclei surface. The high supersaturation coefficient can also be a direct cause of the dendretic shape formation [26,27]. From solution composition, the calculated supersaturation coefficient with respect to pure

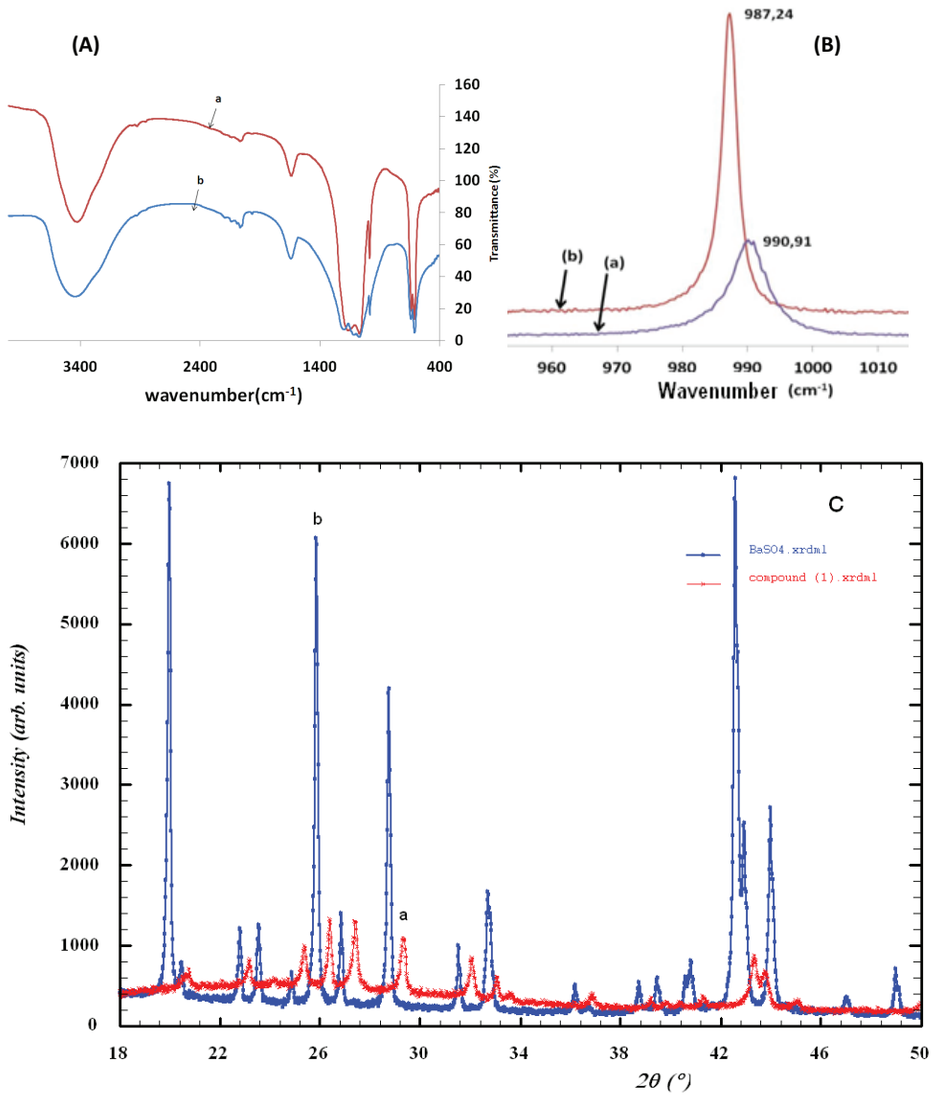

Fig. 4. Analysis of compound (1) (a) and pure $BaSO_4$ (b): (A) Infrared; (B) Raman; (C) XRD patterns.

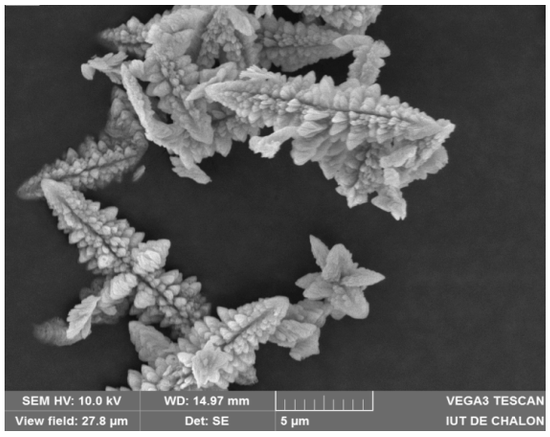

Fig. 5. SEM image of compound (1).

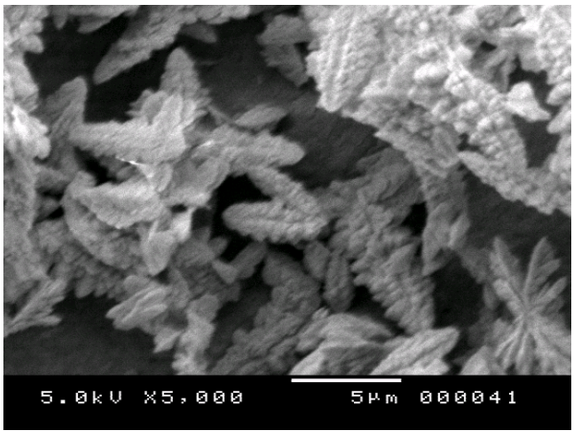

Fig. 6. SEM image of compound (2).

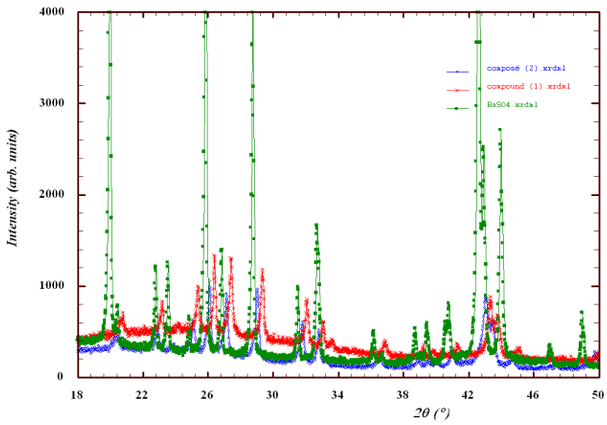

Fig. 7. XRD patterns of the compounds (1), (2) and pure barite.

Table 2
Unit cell parameters and refinements data of compounds (1) and (2)

	$BaSO_4$	Compound (1)	Compound (2)
Crystal system	Orthorhombic	Orthorhombic	Monoclinic
Space Group	*Pmma*	*Pmmm*	*P2/m*
a	10.90	10.51	17.87
b	8.88	8.67	14.14
c	7.15	7.33	4.67
α	90	90	90
β	90	90	96.70
γ	90	90	90
Volume (Å³)	693.00	669.18	1172.56
	Refinement parameters		
Chi 2	9.80	2.95	2.3
R-Factor	3.99	1.83	1.99

Table 3
EDX elemental analyses of compound (1)

Elements	Atomic composition (at.%)	Error (wt.%)
O	65.13	4.1
S	17.30	0.6
Ca	3.58	0.2
Ba	13.99	1.4

barite phase in experiment c (Ω_{BaSO_4}) is about 6×10^4. Considering that the substitution/insertion of calcium led to a slight increase in the solubility of the solid solution of calcium and barium sulfate (%Ca < %Ba) regarding pure barite as for $Ca_{1-x}Mg_xSO_4$ and $Ca_{1-x}Mg_xCO_3$ [28], the supersaturation coefficient regarding the solid solution remains important.

The compound (2), which was recovered at the beginning of the conductivity drop in the precipitation curve, shows similar dendretic morphology as that of the compound one (Fig. 6).

Also, XRD pattern shows the same peaks as those of the compound (1) but not at the same 2θ (Fig. 7).

As for the compound (1), a peak shift regarding barite one was recorded. Nevertheless, this shift was towards lower 2θ (Fig. 8). This lets suggest that:

- For compound (1): for $x < 0.5$, the peak shift is due to the lattice distortions caused by the presence of calcium. Indeed, calcium can be a part of the barite lattice by substituting the Ca ions. This involves a slight compression of the crystal lattice, which results in a decrease of the unit cell volume and a shift of the XRD peaks to higher 2θ angles. The additional peaks and a disappearance of some peaks, which can be attributed to the insertion of Ca^{2+} in the barite lattice.
- For compound (2): $x > 0.5$, the unit cell volume increases. This can be explained by the fact that, in addition to the substitution and insertion of the Ca^{2+}, Ca ions could be adsorbed in the gypsum crystal surfaces. This causes tensile stresses, the origin of the increase of the unit cell volume, and the peak shift to lower 2θ angles [28].

At light of these analyses, it can be concluded that the compound (1) is metastable and transforms to a second compound, usually a solid solution of calcium and barium sulphate. In this compound (2), in addition to substitute barium, calcium insert in the solid solution lattice.

So, compound (1) was crystallized in the same crystal system as pure barite (orthorhombic) and compound (2) was crystallized in almost identical crystal system as gypsum (monoclinic).

In 1970 and in 1972 [19; 29], Vojtěch has presented a detailed study of the structural proprieties of $BaSO_4$-$CaSO_4$ system in the whole concentration range ($0 < x < 1$). It was found that mixed crystals had a barite lattice type (from about 40% mol. $BaSO_4$) and a lattice of the anhydrite type (below 40% mol. $BaSO_4$) formed. This fact can be explained by that it is these substances with $x < 0.5$ that have a structure almost identical with the structure of pure barite.

At the end of the precipitation test, the recovered precipitate (compound (3)), is mainly gypsum as shown by XRD analysis presented in Fig. 9. The XRD patterns is almost the same of that of the gypsum, synthesized at laboratory scale

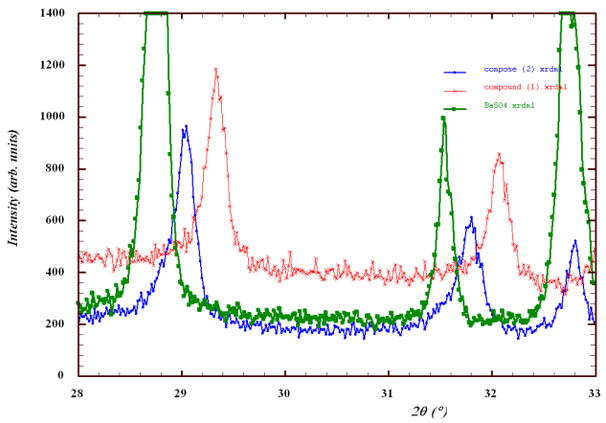

Fig. 8. Additional zoom XRD patterns of the compounds (1), (2) and pure barite.

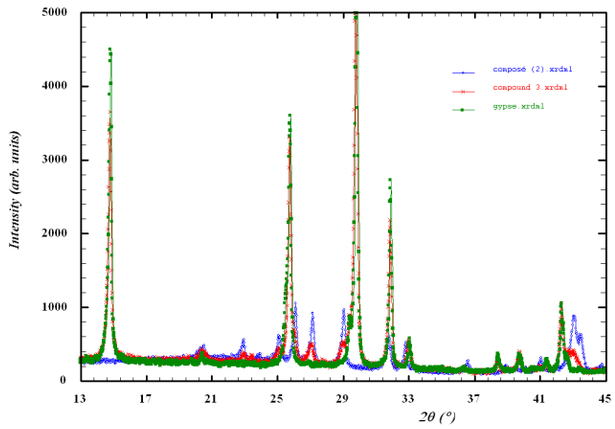

Fig. 9. XRD patterns of compounds (2), (3) and pure gypsum.

as reference; only few additional peaks are recorded at 2θ = 22.92°, 25.08°, 27.12° which belong to compound (2).

From the analysis made of compounds (1), (2) and (3) we can conclude that the simultaneous presence of Ba^{2+}, Ca^{2+} and SO_4^{2-} gave birth to series of intermediate compounds with formula $Ba_{1-x}Ca_xSO_4$. So, the final compound is nearly pure gypsum as a consequence of the reduced barium concentration in solution. At this final stage, there was a formation of gypsum as it was indicated by the XRD spectrum of compound (3) (Fig. 9).

4.2.2. In alkaline medium pH=8.3:

To study the effect of pH on the phenomenon of co-precipitation, experiment (d) was carried out at pH = 8.3. Fig. 10 shows the precipitation curves in the $CaCl_2$-Na_2SO_4-$BaCl_2$ solution in alkaline medium. Barium ion did not present any significant effect on pure gypsum precipitation (the retarding effect disappears). SEM image of the final product (Fig. 11) of the experiment (d) indicates the presence of the barite and gypsum, and the absence of the intermediates compounds (dendritic form). According to the literature,

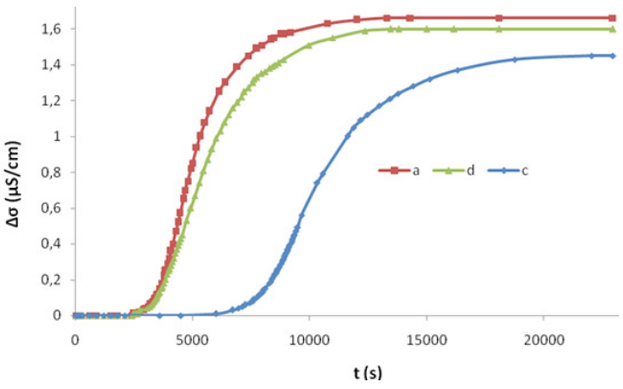

Fig. 10. Temporary delta conductivity variation ($\Delta\sigma = \sigma_{initial} - \sigma_t$) at 303 K in gypsum supersaturated solution with: a) $[Ba^{2+}] = 0$ M at pH = 5.5, c) $[Ba^{2+}] = 10^{-3}$ M at pH = 5.5 and d) $[Ba^{2+}] = 10^{-3}$ M at pH = 8.3 ($\Omega_{gypsum} = 6$, T = 303 K).

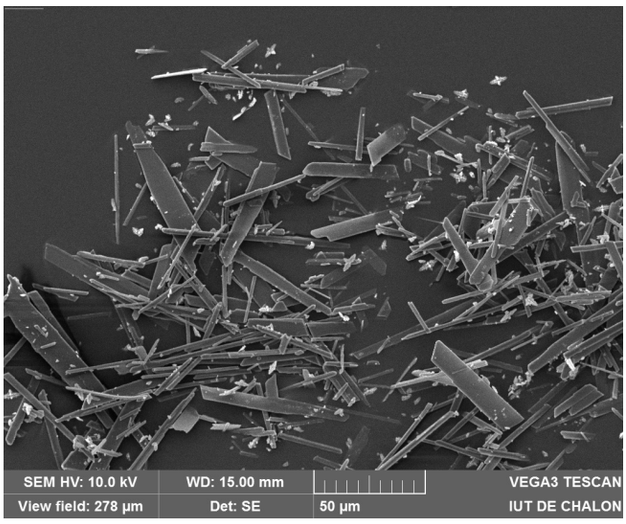

Fig. 11. SEM image of deposit compound obtained at the end of experience (d).

gypsum and barite nucleation are not significantly affected by pH in the range 5–9 [30,31]. Thus, we can attribute this difference in behavior between pH 5.5 and pH = 8.3 to electrostatic interaction between barite and calcium sulphate during the germination step. This difference in electrostatic interaction is explained by the change in zeta potential of the barium as a function of pH. Indeed, at pH = 5.5 barum sulphate have a positive potential and a negative potential at pH = 8.3 [32].

5. Conclusions

The present research is focused on the effect of barium ions on gypsum crystallization in aqueous solutions at an acid and an alkaline pH, based on conductivity measurements and integrated by a morphological and structural investigation (FTIR, RAMAN, SEM and XRD).

The obtained results demonstrated that the presence of barium ions under acid medium results a hindrance of gypsum and the formation of mixed intermediate compound $Ba_{1-x}Ca_xSO_4$ with dendrite morphologic formation. So, we may conclude that $BaSO_4$-$CaSO_4$ co-precipitation is occurring and not a heterogeneous nucleation of gypsum on barite. Probably, the co-precipitation causes a decrease of the supersaturation in respect to gypsum and an increase of its induction time for nucleation.

For *x* lower than 0.5, microstructural analyses showed that XRD peaks shifted to higher 2θ angles and the unit cell volume decreases. It was, therefore, suggested that Calcium ions act by substituting the barium ion and by insertion in the barite lattice.

For *x* beyond 0.5, peaks shifted to lower 2θ angles and the unit cell volume increases by insertion and adsorption of calcium ion in $Ba_{1-x}Ca_xSO_4$ lattice.

At an alkaline medium, Barium ions did not present any significant effect on the pure gypsum precipitation. This difference with respect to the acid medium is assigned to the change in zeta potential of the barium as a function of pH.

Hence, all studies of mediums (solubility, particle size, inhibitor ...) containing Ba^{2+}, Ca^{2+} and SO_4^{2-}, need to consider the difference between intermediate compounds and pure compounds.

References

[1] J. Moghadasi, M. Jamialahmadi, H. Muller-Steinhagen, A. Sharif, A. Ghalambor, R.M. Izadpanah, E. Motaie, January 29–30, Scale formation in Iranian oil reservoir and production equipment during water injection, Proc. 5th International Oilfield Scale Symposium and Exhibition, Aberdeen, UK., 2003, pp. 1–14.

[2] A.B. Bin Merdhah, Inhibition of barium sulphate scale at high-barium formation water, J. Petrol. Sci. Eng., 90–91 (2012) 124–130.

[3] G.A. Moldoveanu, V.G. Papangelakis, Strategies for calcium sulphate scale control in hydrometallurgical processes at 80°C, Hydrometallurgy, 157 (2015) 133–139.

[4] C. Fan, R.M. Pashley, The controlled growth of calcium sulphate dihydrate (gypsum) in aqueous solution using the inhibition effect of a bubble column evaporator, Chem. Eng. Sci., 142 (2016) 23–31.

[5] H. Sudmalis, R. Heikholeslami, Coprecipitation of $CaCO_3$ and $CaSO_4$, Can. J. Chem. Eng., 78 (2000) 21–31.

[6] F. He, K.K. Sirkar, J. Gilron, Studies on scaling of membranes in desalination by direct contact membrane distillation: $CaCO_3$ and mixed $CaCO_3/CaSO_4$ systems, Chem. Eng. Sci., 64(15) (April 2009) 1844–1859.

[7] X. Liu, T. Chen, P. Chen, H. Montgomerie, T. Hagen, B. Wang, X. Yang, Understanding the co-deposition of calcium sulphate and barium sulphate and developing environmental acceptable scale inhibitors applied in HTHP wells, Paper presented at the SPE International Conference and Exhibition on Oilfield. Scale, Aberdeen, UK, May 30–31, 2012, Paper No. 156013.

[8] Y. Zarga, H. Ben Boubaker, N. Ghaffour, H. Elfil, Study of calcium carbonate and sulphate co-precipitation, Chem. Eng. Sci., 96 (2013) 33–34.

[9] J. Mulopo, Continuous pilot scale assessment of the alkaline barium calcium desalination process for acid mine drainage treatment, J. Environ. Chem. Eng., 3 (2015) 1295–1302.

[10] C. ZHU, Coprecipitation in the Barite Isostructural Family: 1, Binary Mixing Properties, Geochim. Cosmochim. Acta., 68(16) (2004) 3327–3337.

[11] S.Naseri, J. Moghadasi, M. Jamialahmadi, Effect of temperature and calcium ion concentration on permeability reduction due to composite barium and calcium sulphate precipitation in porous media, J. Nat. Gas Eng., 22 (2015) 299–312.

[12] J. Rodriguez-Carvajal, FULLPROF: A Program for Rietveld Refinement and Pattern Matching Analysis, Abstracts of the Satellite Meeting on Powder Diffraction of the XV Congress of the IUCr, p. 127, Toulouse, France (1990).

[13] W.L. Marshall, R. Slusher, Thermodynamics of calcium sulphate dehydrate in aqueous sodium chloride solution, 0–100 1C. J. Phys. Chem., 70 (1966) 4015.

[14] C. Monnin, A thermodynamic model for the solubility of barite and celestite in electrolyte solutions and seawater to 2008C and to 1 kbar, Chem. Geol., 153 (1999) 187–209.

[15] L.W. Davies, Ion Association, Butterworths, London (1962).

[16] V. Ramaswamy, R.M. Vimalathithan, V. Ponnusamy, Synthesis and characterization of $BaSO_4$ nano particles using micro emulsion technique, Adv. Appl. Sci. Res., 1 (2010) 197–204.

[17] M.M. Tlili, M. Ben Amor, C. Gabrielli, S. Joiret, G. Maurin, P. Rousseau, Study of Electrochemical Deposition of $CaCO_3$ by *In Situ* Raman Spectroscopy : II. Influence of the Solution CompositionELECTROCHEMICAL/CHEMICAL DEPOSITION AND ETCHING, J. Electrochem. Soc. 150 (2003) 485–493.

[18] C. Yen-Hua, H. Eugene, Y. Shu-Cheng, High-pressure Raman study on the $BaSO_4$–$SrSO_4$ series, Solid. State. Commun., 149 (2009) 2050–2052.

[19] O. Vojtěch, J. Moravec, F. Volf, M. Dlouhá, $BaSO_4$-$CaSO_4$ solid solutions isotypic with $BaSO_4$, J. Inorg. Nucl. Chem., 32 (1970) 3725.

[20] N. Sánchez-Pastor, C.M. Pina, L. Fernández-Díaz, Relationships between crystal morphology and composition in the (Ba,Sr)SO_4–H_2O solid solution–aqueous solution system, Chem. Geol., 225 (2006) 266–277.

[21] F. Jones, P. Jones, M.I. Ogden, W.R. Richmond, A.L. Rohl, M. Saunders, The interaction of EDTA with barium sulphate, J. Colloid. Interf. Sci., 316 (2007) 553–561.

[22] E. Brener, I.V. Melnikov, Pattern selection in two-dimensional dendritic growth, Adv. Phys., 40 (1991) 53–97.

[23] Y. Pomeau, M. Ben Amar, Dendritic growth and related topics in Solids far from equilibrium, ed. C. Godrèche, Cambridge 1991, pp. 365–431.

[24] W. Kurz, R. Trivedi, Solidification microstructures: Recent developments and future directions, Overview No. 87. Acta. Metall. Mater., 38 (1990) 1–17.

[25] D. Kessler, J. Koplik, H. Levine, Patterned selection in fingered growth phenomena, Adv. Phys., 37 (1988) 255–339.

[26] S. Senouci, A.A. Raho, L'influence de la sursaturation sur la cinétique des zones GP dans les alliages Al-Ag à Température de 200°C, 3éme Conférence international sur le sodage et l'industrie des matériaux et alliages, Alger (2012).

[27] S. Goldsztaub, R. Kern, Etude de la concentration de la solution autour d'un cristal en voie de croissance, Acta. Cryst., 6 (1953) 842–845.

[28] S. Ben Ahmed, M.M. Tlili, M. Amami, M. Ben Amor, Gypsum precipitation kinetics and solubility in the NaCl–$MgCl_2$–$CaSO_4$–H_2O System, Ind. Eng. Chem. Res., 53 (2014) 9554–9560.

[29] O. Votěch, H. Selucká, Stroncium sorption on the sorbents of $BaSO_4$-$CaSO_4$ system, ÚJV 2820.Ch. ŘEž, Nuclear Research Institute, Information Center (1972).

[30] C. Ruiz-Agudo, C.V. Putnis, E. Ruiz-Agudo, A. Putnis, The influence of pH on barite nucleation and growth, Chem. Geol., 391 (2015) 7–18.

[31] J. Shukla, V.P. Mohandas, A. Kumar, Effect of pH on the solubility of $CaSO_4 \cdot 2H_2O$ in aqueous NaCl Solutions and physicochemical solution properties at 35°C, J. Chem. Eng. Data., 53 (2008) 2797–2800.

[32] J. Hang, L. Shi, X. Feng, L. Xiao, Electrostatic and electrosteric stabilization of aqueous suspensions of barite nanoparticles, Powder. Technol., 192 (2009) 166–170.